a reprint from Applied Optics

Detection of neutral and ionic reaction mechanisms in molecular clusters

Jhobe Steadman, Eric W. Fournier, and Jack A. Syage

Techniques based on picosecond resonance-enhanced multiphoton ionization and mass-selective ion photodissociation are described as a means for studying complex reaction mechanisms in molecular clusters. A set of experiments is described that can identify the cluster-size specific reactions that occur by the overlapping processes of neutral dissociation/fragment ionization, parent ionization/dissociation, and parent ion photoexcitation/dissociation. These molecular beam techniques are demonstrated for the case of neutral and ionic photon transfer and evaporation in clusters of phenol in $(NH_3)_n$, as well for radical chemistry and van der Waals dissociation in $(CH_3I)_n$ clusters. *Key words:* Cluster reactions, picosecond spectroscopy, ionization, ion photodissociation, molecular beams, mass spectrometry.

I. Introduction

Multiphoton ionization (MPI) is a very energetic process in which the total number of photons absorbed by a molecule or cluster is sometimes difficult to control. Consequently, it is common to observe extensive fragmentation of the species under study.[1–3] A number of possibilities can be envisioned to describe the mechanism of fragmentation in MPI excitation. At any stage of the multiphoton absorption process, the molecule can either absorb another photon (ladder climbing) or dissociate to form a fragment (ladder switching), which in turn can absorb photons and ionize or further dissociate to secondary fragments. Unraveling the fragmentation mechanism has constituted a prominent field of study for some years.[1–5]

The study of chemical reactions in molecular clusters is a rapidly expanding field of research that relies strongly on MPI mass spectrometry for understanding the dependence of reactivity on cluster size.[6–15] The formidable task of distinguishing between the different channels that can produce a single fragment ion signal from a single parent molecule becomes even more complex for cluster fragmentation because now one begins with a distribution of cluster sizes. Figure 1 shows that even in the simplest representation there can be multiple pathways for production of a detected fragment ion. We consider three basic processes corresponding to (1) dissociation from an intermediate neutral excited state and fragment ionization, (2) parent ionization followed by dissociation, and (3) parent ionization followed by photoexcitation and dissociation. Whereas procedures have been reported to differentiate neutral and ionic fragmentation patterns from single starting molecules,[1–5] no satisfactory means exists for unraveling the overlapping processes from a distribution of cluster species.

In this paper, we describe two complementary laser molecular beam mass spectrometric techniques that enable the selective detection of ion fragments formed from clusters by the various possible pathways outlined in Fig. 1. The first method makes use of picosecond pump-probe excitation/ionization to distinguish specific pathways on the basis of the time dependences observed for the intensity of the product ion signal. The picosecond approach is particularly well suited for studying rapid neutral cluster chemistry.[11–15] The second method is based on direct ionization in concert with a new technique for recording mass-selective ion photodissociation spectra.[16,17] This strategy identifies the ground and electronically excited cluster ion dissociation mechanisms.

II. Experimental

A. Molecular Beam

The molecular beam time-of-flight (TOF) mass spectrometer apparatus is a conventional differentially pumped two chamber system. The vacuum apparatus and associated components are represented in Fig.

The authors are with Aerospace Corporation, Aerophysics Laboratory, P.O. Box 92957, Los Angeles, California 90009.

Received 12 March 1990.
0003-6935/90/334962-07$02.00/0.

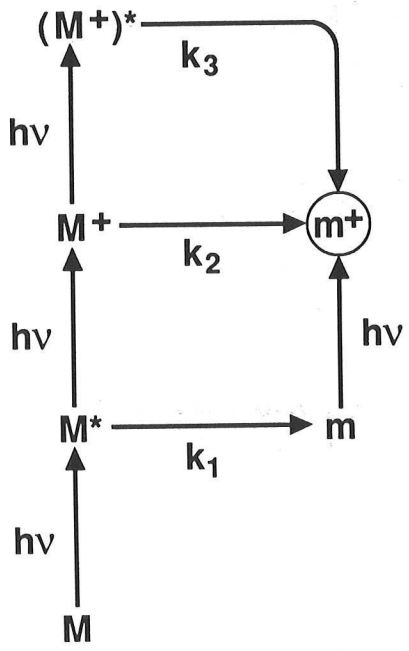

Fig. 1. A simple representation of ladder climbing and ladder switching mechanisms for multiphoton-ionization-dissociation that considers three processes: (1) dissociation from an intermediate neutral excited state and fragment ionization, (2) parent ionization followed by dissociation, and (3) parent ionization followed by photoexcitation and dissociation.

2 and are described in detail elsewhere.[10] Typical pulsed expansion conditions were 35-psi He or Ar, 500-μm nozzle diam, 400-μs pulse width, 2-cm nozzle-skimmer distance, and 1-mm diam skimmer. The ambient base pressure in the ionization chamber was typically 3 $\times 10^{-8}$ Torr, rising about 2×10^{-7} Torr during operation of the pulsed nozzle at 10 Hz. The ion optics are comprised of the usual three grids for space focussed ion acceleration,[18] and is equipped with a pulsed electron impact (EI) ionization source.[19] The residence time of ions in the ion optics assembly depends on mass and whether a delayed extraction pulse is used, however, the range is typically 1–5 μs.

Molecular clusters were prepared by a variety of procedures. For solvated phenol, the aromatic compound was placed in a removable sample holder mounted in a temperature-controlled pulsed nozzle (we used 60 °C for phenol). In the case of ammonia solvation, a 2-liter high-pressure cylinder was made up containing 10% ammonia in helium which was used as the carrier gas. For the CH_3I studies, the sample was prepared by flowing Ar (20–30 psi) through a bubbler that was cooled in a bath of dry ice/acetone or ice water, depending on the extent of clustering desired.

B. Cluster Ion Photodissociation

Ion photodissociation experiments made use of a crossed electron-laser-molecular beam configuration.[16,17] In one adaptation, neutral clusters were directly ionized by EI excitation and the cluster ions resonantly photodissociated using nanosecond laser pulses. Mass-selective photoexcitation and product ion detection were performed using a new technique in which a time-of-flight (TOF) mass spectrometer was operated as a low mass rejection filter. The specific details of this device are provided elsewhere,[16] however, the basic concept is as follows. The molecular beam pulse is first ionized by EI excitation under field-free conditions. A positive voltage pulsed is then applied to the extraction grid (the second grid in the

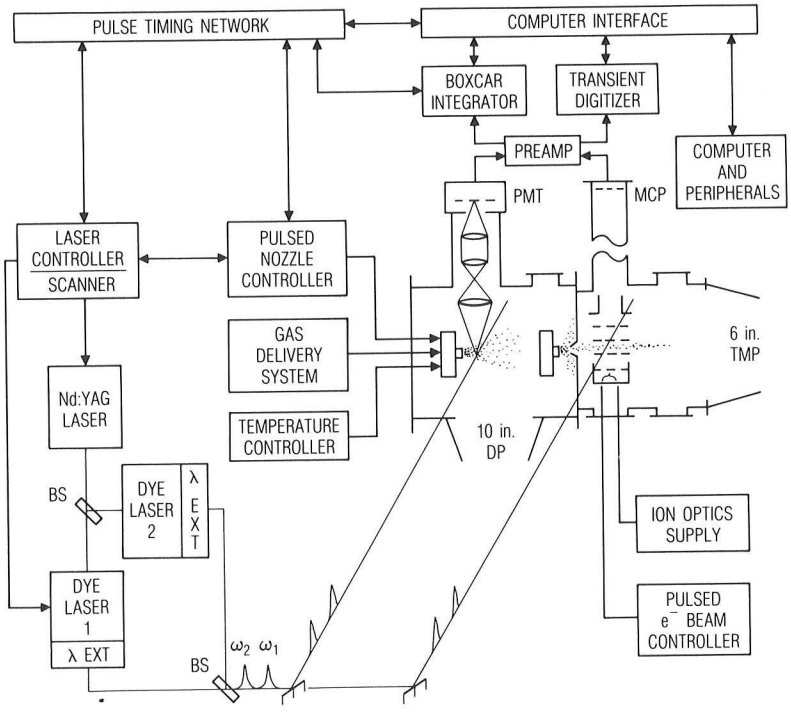

Fig. 2. Schematic of the experimental apparatus. In the present work, 2-C excitation was achieved using a single dye laser and the second, third, or fourth harmonic of the Nd:YAG laser. Symbols are defined as follows: *MCP* = microchannel plate detector; PMT = photomultiplier tube; *TMP* = turbomolecular pump; *DP* = diffusion pump; *BS* = beam splitter; λ *EXT* = wavelength extension components. Free jet fluorescence detection was not used in the present study.

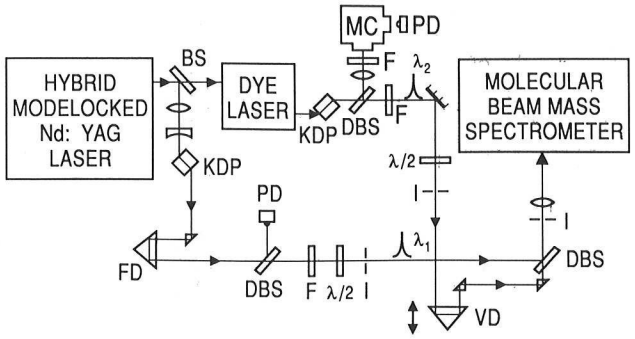

Fig. 3. A typical picosecond pump-probe configuration involving the use of Nd:YAG harmonics and a tunable dye laser. Terms are defined as follows: *BS*, beam splitter; *DBS*, dichroic beam splitter; *F*, filter; *FD*, fixed delay line; *I*, iris, $\lambda/2$, halfwave plate; *MC*, monochromator; *PD*, photodiode; *VD*, variable delay line.

three-grid TOF ion optics assembly) to create a potential gradient (field) across the ionization region that accelerates the ions away from the detector. This is followed by a positive pulsed applied to the repeller grid which reverses the direction of the ions toward the detector. A range of lighter masses, having traveled further than the heavier masses during the initial acceleration period, will not be able to complete the turn before exiting the lower repeller grid, and are therefore rejected. The heavier masses that have not escaped the grid region are accelerated toward the detector to give a TOF mass spectrum with the primary low ion masses filtered out. If a delayed laser pulse is introduced after the heavier ions have turned around, then photodissociation may occur with the resultant photofragments appearing in the mass spectrum against a zero background. Successively larger cluster ions can be filtered out before photodissociation, thus providing a means for recording size-selective cluster ion photodissociation spectra.

C. Picosecond Pump-Probe

A pulsed (10 Hz) active/passive mode-locked and amplified Nd:YAG laser was used to introduce frequency doubled (532 nm, 25 ps), tripled (355 nm, 25 ps), and quadrupled (266 nm, 18 ps) output, and to pump a short-cavity tunable dye laser (10 ps).[14,15] A typical optical set-up is illustrated in Fig. 3. The pump excitation was usually provided by 266-nm pulses or frequency-doubled dye laser pulses. The probe excitation was supplied by either the 532-nm or 355-nm Nd:YAG harmonics, or by the dye laser fundamental and/or frequency doubled output. In the latter case, the doubled Nd:YAG output (532 nm, 25 ps, 20 mJ) was split into equal portions to pump the dye laser (580–600 nm, 10 ps, 0.5–1.0 mJ) and a doubling crystal (266 nm, $\sim$ 0.4 mJ). The λ_1 and the λ_2 pulses traveled along separate variable delay lines and were then combined using a dichroic beamsplitter and directed collinearly into the molecular beam apparatus. Polarizing attenuators and neutral density filters were used to reduce pulse energies. Time-resolved spectra were recorded by delaying the probe pulse λ_2 relative to the pump pulse λ_1 using a scanning optical delay line. The nominal time resolution, was measured by the 20–80% risetime for two-color ionization was 20 ps. The recorded time-resolved traces were typically reproducible within the noise level and permitted time-constant measurements to better than 10 ps using a curve fitting and pulse-width convolution program.

III. Picosecond Time-Resolved Selectivity

Because the various reaction pathways leading to a specific fragment ion signal (m^+ in Fig. 1) usually proceed at different rates, time-resolved spectroscopy can assist in sorting out the relative contributions of each channel. The following scheme illustrates how a two-pulse picosecond sequence consisting of a pump pulse (λ_1) and a probe pulse (λ_2) delayed by time t can distinguish between neutral and ionic channels. We consider in Scheme I (Fig. 4, top) processes (1) and (2) from Fig. 1. The subscripts s and c refer to ladder switching (neutral) and ladder climbing (ionic), respectively. If one assumes that the initially excited molecule or cluster M^* decays solely by dissociation to m, with a rate k_s, then it follows that the contributions to the m^+ ion signal from the neutral ladder switching and ionic ladder climbing channels, $I_s(t)$ and $I_c(t)$, respectively, are described by

$$I_s(t) = A_s[1 - \exp(-k_s t)], \tag{1}$$

$$I_c(t) = A_c \exp(-k_s t) \tag{2}$$

$$I(t) = I_s(t) + I_c(t), \tag{3}$$

where t is the time delay between the preparation of M^* (by pulse λ_1) and the subsequent ionization (by pulse λ_2). The coefficient A_s is a function of the ionization cross-section σ_s, and A_c is a function of σ_c and k_c (k_c determines how much parent ion dissociation occurs over the residence time of the mass spectrometer). The observed ion signal $I(t)$ for m^+ consists of the sum of I_s and I_c [Eq. (3)]. The time dependence for clusters may be more complicated because a specific product ion may originate from different initial cluster sizes due to multiple reactions or evaporation. For the sake of simplicity, we assume that the time dependences for clusters are adequately described by Eqs. (1)–(3), and that the A coefficients represent the sum over different cluster sizes contributing to the same detected signal.

In previous work we employed picosecond pump–probe pulse sequences to measure fast neutral cluster reactions.[14,15] Here, we demonstrate that useful information regarding the ionic dissociation mechanism may also be obtained. We consider below the prototypical excited state proton transfer reaction of phenol to a solvent cluster of sufficient basicity to promote reaction. The excitation and kinetic steps are represented in Scheme II (Fig. 4, bottom). For the results presented herein, λ_1 = 266 nm excites phenol to the first excited electronic state S_1. Depending on the $(NH_3)_n$ solvent cluster size n, a proton transfer can occur with a rate constant k_s. The probe pulse λ_2

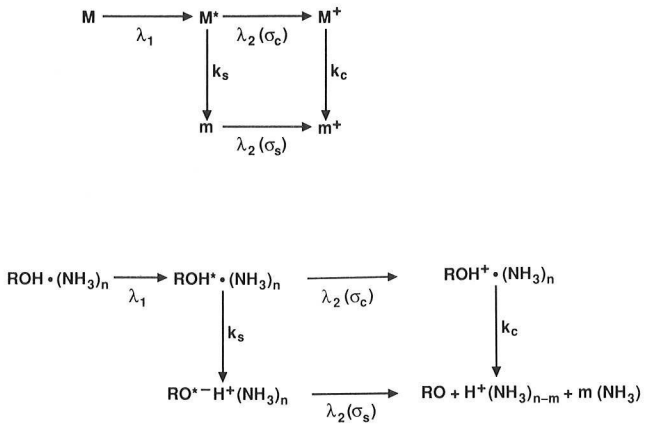

Fig. 4. Scheme I (top) and Scheme II (below).

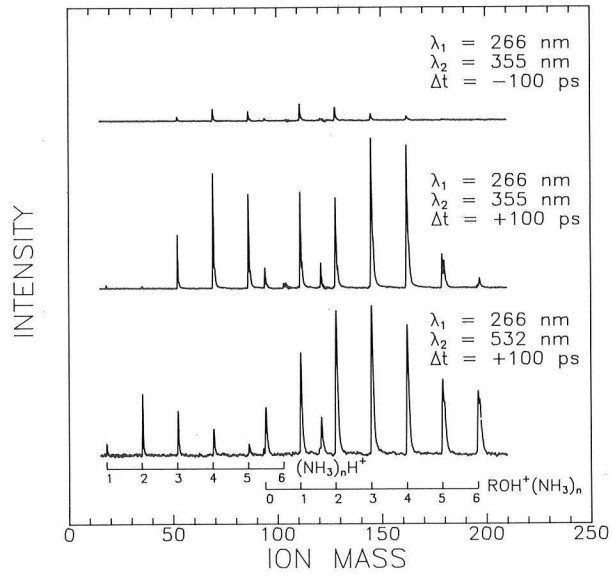

Fig. 5. Picosecond pump-probe mass spectra of phenol-$(NH_3)_n$ as a function of different relative delay times and probe wavelengths. The signal at mass 121 is an unidentified impurity.

ionizes the reactant ROH* · $(NH_3)_n$ and product RO*− · $H^+(NH_3)_n$ clusters as a function of time. Two-photon ionization at $\lambda_2 = 532$ nm or one-photon ionization at $\lambda_2 = 355$ nm was used for probe excitation. As shown above, dissociation of the parent ion and ionization of neutral product may produce the same ion signal. Reactions from different cluster sizes n may also contribute to the same signal $H^+(NH_3)_{n-m}$, further obscuring the chemistry. Inspection of the REMPI mass spectra and analysis of the product ion time-dependences can provide the necessary information to unravel the multitude of processes.

The picosecond pump-probe mass spectra in Fig. 5, shown as a function of $\lambda_1 - t - \lambda_2$ delay time t and the wavelength λ_2, reveal a large number of reactant and product signals. Because the proton transfer reaction from S_1 phenol depends on the proton affinity of the

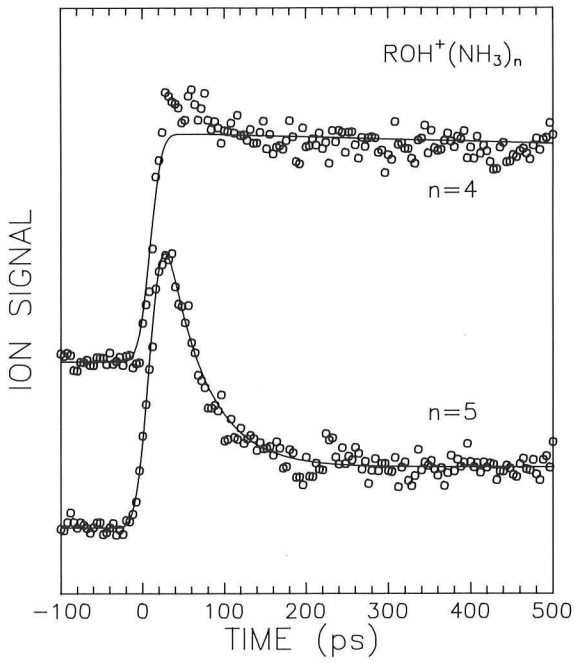

Fig. 6. Time-resolved measurements of reactant cluster ROH* · $(NH_3)_n$ [as detected by the ion signal $ROH^+ \cdot (NH_3)_n$] showing onset to reaction at $n = 5$. The calculated curves, based on a simple model (Ref. 15), are included for clarity.

solvent cluster,[20,21] the reaction only occurs when $(NH_3)_n$ reaches a requisite size. This is amply demonstrated in Fig. 6, in which a distinct onset for a 65 ± 10 ps decay of ROH* · $(NH_3)_n$ occurs in going from a solvent cluster size of $n = 4$ to $n = 5$. This level of solvation marks the point at which the reaction becomes exothermic.

The detected $(NH_3)_nH^+$ signals in Fig. 7 result from dissociative ionization of reactant ROH* · $(NH_3)_n$ and product RO*− · $H^+(NH_3)_n$ clusters by the probe pulse λ_2 as outlined in scheme II.[15] We note that the time dependences show differences that depend on cluster size n and ionization wavelength λ_2. Because Fig. 6 reveals that the reaction rate constant k_s only becomes significant for $n \geq 5$, the time dependences for the $(NH_3)_nH^+$ signals ($n < 5$) should not contain a contribution from the neutral k_s channel (unless evaporation, discussed below, occurs). No signal due to $(NH_3)_nH^+$ for $n = 1,2$ was observed using $\lambda_2 = 355$ nm (Fig. 5), indicating that k_s (from ladder switching) and k_c (from ladder climbing) are immeasurably small. The $(NH_3)_nH^+$ $n = 1$ signal by $\lambda_2 = 532$ nm ionization [Fig. 7(a)] exhibits a step function dependence, which according to Eq. (2) occurs when $1/k_s$ is long relative to the picosecond measurement time period (and $1/k_c$ is less than the mass spectrometer residence time). The calculated curves through the data include a convolution with the system response function. For larger values of n, a new contribution to $(NH_3)_nH^+$ grows in at a rate that closely matches the 65-ps decay time of the reactant in Fig. 6. For $n \geq 3$ in Fig. 7, contributions to $(NH_3)_nH^+$ by both the neutral and ionic channel can be

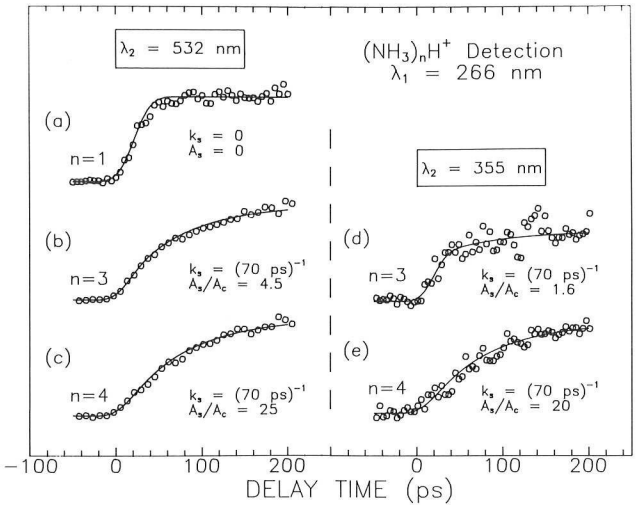

Fig. 7. Time-resolved measurements of product formation by detecting the ion signal $(NH_3)_nH^+$ for two different λ_2 probe wavelengths. Calculated curves [Eqs. (1)–(3)] reflect the relative amount of signal occurring by ladder climbing versus ladder switching processes. A greater amount of evaporation occurs by the ladder switching. The calculations all assumed a value of $k_s = (70\ \text{ps})^{-1}$.

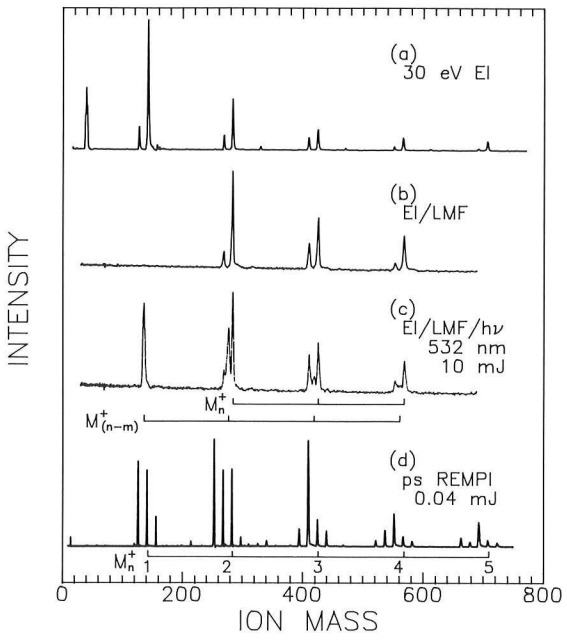

Fig. 8. $(CH_3I)_n$ cluster ionization mass spectra ($M = CH_3I$): (a) direct ionization by EI excitation at 30 eV; (b) EI ionization and low mass filter (LMF); (c) same, but with resonant photodissociation of cluster ions; and (d) Picosecond Ã state REMPI. Expansion conditions were 5% CH_3I in 1200 torr Ar.

discerned in relative amounts that are proportional to the ratio A_s/A_c. This ratio is observed to be large when the neutral reaction occurs indicating that $(NH_3)_nH^+$ is produced more efficiently by ionization from the ion pair form $RO^{*-} \cdot H^+(NH_3)_n$ than from the reactant form $ROH^* \cdot (NH_3)_n$. We presume that this property is due to the increased energy available for dissociation when ionization occurs from the proton transfer (ion pair) complex, which has a lower ionization potential (by ~1 eV)[22] than the excited neutral reactant.

Finally, we note that evaporation of NH_3 solvent from the reactant and product ion signals can be detected in the picosecond measurements. Evaporation from the reactant species $ROH^* \cdot (NH_3)_n$ and $ROH^+ \cdot (NH_3)_n$ has been found to be minor under our excitation conditions on the basis of the following evidence: (1) The $ROH^+ \cdot (NH_3)_n$ signal intensity in Fig. 5 is much greater for $n = 1$ than it is for $n = 0$ indicating that the former does not significantly decay to the latter by evaporation, and (2) there is only a negligible residual (~10%) of the $n = 5$ decay dependence superimposed on the step function response for $n = 4$ in Fig. 6. Evaporation does occur extensively in the product species $(NH_3)_nH^+$ formed by the neutral ladder switching channel. Whereas the onset to neutral reaction is known to ocur at $n = 5$ (Fig. 6), the $(NH_3)_nH^+$ formation signal reveals a neutral channel contribution growing in at $n = 3$ in Fig. 7(b). Hence, the relative value of A_s in Figs. 7(b) and (c) has a large component due to evaporation from the $n \geq 5$ neutral reaction channel. Apparently, for two-photon ionization at $\lambda_2 = 532$ nm, two NH_3 molecules can dissociate as a result of the excess ion energy. For the less energetic one-photon ionization at $\lambda_2 = 355$ nm, the neutral channel only becomes prominent at $n = 4$ (Figs. 6(d) and (e) indicating a loss of one NH_3 molecule.

The results in this section can be summarized as follows: (1) the cluster size thresholds for neutral excited state and ionic ground state proton transfer are $n = 5$ (k_s) and $n = 3$ (k_c), respectively; (2) $ROH^+ \cdot (NH_3)_n$ and, to a lesser extent, $(NH_3)_nH^+$, formed by the ladder climbing route, do not undergo significant evaporation for any of the ionizing probe λ_2 wavelengths used; (3) $(NH_3)_nH^+$ formed by the neutral ladder switching route undergoes evaporation in the ion of one or two NH_3 molecules depending on the photon energy of ionization.

IV. Direct Ionization and Mass-Selected Ion Photodissociation

In this section we describe experiments that permit the independent measurement of ion dissociation mechanisms by using direct electron-impact (EI) ionization followed by mass-selective ion photodissociation. The ion photodissociation experiments make use of the crossed electron-laser-molecular beam configuration described in Sec. II.B. The molecular clusters are first ionized by EI excitation, then mass filtered, and finally resonantly photodissociated using nanosecond laser pulses. Unlike other mass-selected photofragmentation techniques, which rely on tandem mass spectrometer designs,[23] the method employed here can be adapted to any conventional three-grid TOF mass spectrometer (Sec. II.B).

The principle behind using both picosecond REMPI and direct ionization/photodissociation to identify neutral cluster reactions is illustrated in Fig. 8 for $(CH_3I)_n$ clusters. The EI mass spectrum in Fig. 8(a)

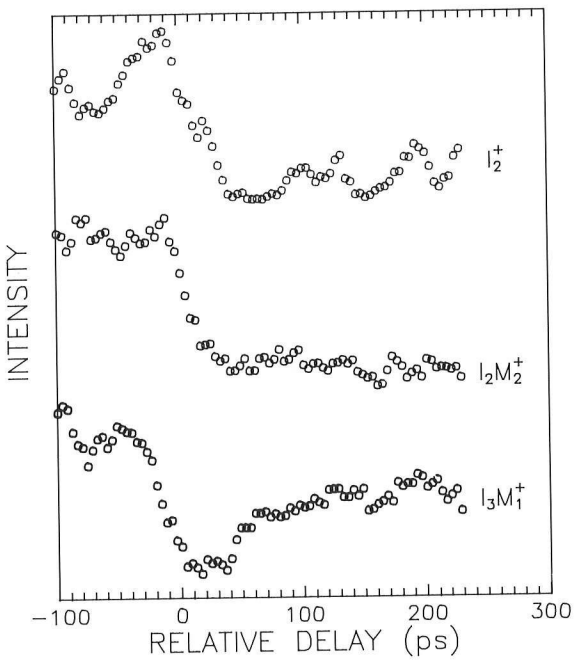

Fig. 9. Picosecond measurements using 266-nm pump and 532-nm probe: M_n ($M = CH_3I$) reaction for loss of two and three CH_3 groups [I_2M_{n-2} (n = 2–4) and I_3M_{n-3} (n = 4), respectively].

shows ion signals that occur exclusively by ion dissociation processes. The electron beam flux is sufficiently low that only single electron collisions occurs. The estimated ionization probability is about 10^{-6}. Consequently, the ion signals that appear in Fig. 8(a) are due to direct ionization of the parent clusters, which depending on the electron energy, can impart sufficient excess energy to cause ion dissociation. For the conditions of Fig. 8(a), only dissociation of a single C–I bond and/or van der Waals (vdW) evaporation occurs. At low electron energies (<20 eV), these processes become relatively minor for $(CH_3I)_n$ and the mass spectrum is then dominated by parent cluster ions. Photoexcitation of the parent cluster ions leads to channel [3] dissociation in Fig. 1. We employ the TOF low mass filter (LMF), described in Sec. II.B, to measure ion photodissociation as a function of cluster size. The advantage of this device is evident in Fig. 8(b), which shows that ions with mass less than the dimer mass have been rejected from the excitation volume. In Fig. 8(c), low mass rejection is followed by $\tilde{A} \leftarrow \tilde{X}(^2\Pi_{1/2})$ excitation in CH_3I^+. The monomer cation is known to predissociate to $CH_3^+ + I$.[17] The observed mass spectrum for excitation of $(CH_3I)_n^+$ cluster ions, on the other hand, clearly shows that only vdW dissociation occurs rather than C–I bond breaking.

The one-color (λ_1) picosecond REMPI mass spectrum of $(CH_3I)_n$ in Fig. 8(d) exhibits distinctly different features as compared to the direct ionization/cluster ion photodissociation spectra in Figs. 8(a)–(c). The identification of the ionic reaction mechanisms in the latter spectra enables us to assign with confidence the additional fragment signals in Fig. 8(d) to ionization of neutral reaction products. The picosecond REMPI excitations reveal mass signals corresponding to extensive loss of methyl groups, which are reactions that do not occur by the ionic mechanisms recorded in Figs. 8(a)–(c). This assignment is confirmed by two-color pump-probe ($\lambda_1 - t - \lambda_2$) measurements. We present the time-dependence for signals corresponding to loss of two or three CH_3 groups in Fig. 9. A more complete set of data has been reported elsewhere.[14] The photoreactions in $(CH_3I)_n$ were initiated by exciting into the directly dissociative $\tilde{A}$ state by λ_1 = 266-nm excitation and probing for the extent of reaction by varying the λ_2 = 532-nm delay time. The monomer reaction dissociates into $CH_3 + I$ in less than 1 ps,[24] however, in clusters one might expect sufficient caging of the initially formed radicals to induce chemistry. Previous nanosecond MPI studies of $(CH_3I)_n$ clusters[25] failed to reveal most of the rapid chemistry evident in Fig. 8(d).

The measured time dependences in Fig. 9 for the formation of $I_2(CH_3I)_{n-2}$ as a function of cluster size n exhibit a sharp reduction in signal at $t = 0$ and remains at a constant level out to long delay times. The latter behavior is probably due to dissociation by λ_2 of I_2 (or I_2^+) in the long-lived ion, $I_2(CH_3I)_{n-2}^+$. The important feature, though, is the sharp threshold, which indicates that the neutral product giving rise to the ion signal is formed rapidly (within the instrument resolution of 10 ps). Also shown in Fig. 9 is the product $I_3(CH_3I)_{n-3}$, corresponding to loss of three CH_3 groups, that opens up for cluster sizes $n \geq 4$. The ion signal undergoes a rapid response-time-limited depletion at $t = 0$ that recovers for $t > 0$. Because the signal recovers in intensity, it is unlikely that the dissociation occurs in the long-lived ion, but rather in the short-lived neutral. The $I_3M_{n-3}^+$ response is, therefore, strong evidence for a neutral reaction mechanism.

V. Conclusion

The combination of picosecond REMPI and direct ion photodissociation studies holds great promise for studying complex reaction mechanisms in size-specific neutral and ionic clusters. Small molecular clusters represent an uncommon state of matter that is neither gas phase nor condensed phase. Hence, the study of cluster properties as a function of aggregate size can probe the approach to bulk phase behavior on a molecular level of understanding. The molecular beam ionization techniques advocated in this paper are intended to provide a means for elucidating complex reaction mechanisms that can occur in clusters.

This work was funded by the Aerospace Sponsored Research program.

References

1. D. A. Gobeli, J. J. Yang, and M. A. El-Sayed, "Laser Multiphoton Ionization-Dissociation Mass Spectrometry," Chem. Rev. **85**, 529–554 (1985).
2. H. Reisler and C. Wittig, "Multiphoton Ionization of Gaseous Molecules," in *Photodissociation and Photoionization*, K. P. Lawley, Ed. (Wiley, New York, 1985), 1–29.

3. J. A. Syage and J. E. Wessel, "Molecular Multiphoton Ionization and Ion Fragmentation Spectroscopy," Appl. Spectrosc. Rev. **24,** 1–79 (1988).
4. D. A. Lichtin, R. B. Bernstein, and K. R. Newton, "Experimental Appraisal of the Maximal-Entropy Theory of Multiphoton Ionization-Fragmentation," J. Chem. Phys. **75,** 5728–1734 (1981); J. Silberstein and R. D. Levine, "Statistical Fragmentation Patterns in Multiphoton Ionization: A Comparison with Experiment," J. Chem. Phys. **75,** 5735–5743 (1981).
5. U. Boesl, H. J. Neusser, and E. W. Schlag, "Visible and UV Multiphoton Ionization and Fragmentation of Polyatomic Molecules," J. Chem. Phys. **72,** 4237–4333 (1980); J. T. Meek, R. K. Jones, and J. P. Reilly, "Photoelectron Energy Distribution Following UV Laser Ionization of Gas Phase Benzene," J. Chem. Phys. **73,** 3503–3505 (1980).
6. J. F. Garvey and R. B. Bernstein, "Observation of Intramolecular Ion-Molecule Reactions With Ionized Clusters: Hetero Systems . . .," J. Am. Chem. Soc. **109,** 1921–1934 (1987); J. F. Garvey and R. B. Bernstein, "Observation of Intramolecular Ion-Molecule Reactions Within Ionized Clusters: The Methyl Halide Systems," J. Phys. Chem. **90,** 3577–3583 (1986).
7. O. Cheshnovsky, and S. Leutwyler, "Photon Transfer in Neutral Gas-Phase Clusters: α-Naphthol · $(NH_3)_n$," J. Chem. Phys. **88,** 4127–4138 (1988)—"Excited State Photon Trasfer in Neutral Microsolvent Clusters: α-Naphthol · $(NH_3)_n$," Chem. Phys. Lett. **121,** 1–8 (1985).
8. J. J. Breen, W.-B. Tzeng, K. Kilgore, R. G. Keesee, and A. W. Castleman, Jr., "Intracluster Reactions in Phenylacetylene Ammonia Clusters Initiated Through Resonant Enhanced Ionization" J. Chem. Phys. **90,** 19–24 (1989); O. Echt, P. D. Dao, S. Morgan, and A. W. Castleman, Jr., "Multiphoton Ionization of Ammonia Clusters and the Dissociation Dynamics of Protonated Cluster Ions," J. Chem. Phys. **82,** 4076–4085 (1985).
9. B. Brutschy, C. Janes, and J. Eggert, "Intracluster Photon-Transfer Between Methylsubstituted Benzene Cations and Polar Solvent Molecules Studied by Resonant Two-Photon Ionization," Ber. Bunsenges, Phys. Chem. **92,** 74–81 (1988).
10. J. A. Syage, "Reactivity of Aniline Cation to Stepwise Solvation in Hydrogen-Bonded Molecular Clusters," J. Phys. Chem. **93,** 170–179 (1989).
11. D. Ray, N. E. Levinger, J. M. Papanikolas, and W. C. Lineberger, "Time-Resolved Measurements of the Photodissociation and Recombination Dynamics of I_2^- in Mass Selected Cluster Ions," J. Chem. Phys. **91,** 6533 (1989).
12. J. J. Breen, L. W. Peng, D. M. Willberg, A. Heikal, P. Cong, and A. H. Zewail, "Real-Time Probing of Reactions in Clusters," J. Chemn. Phys. **92,** 805–807 (1990).
13. J. L. Knee, L. R. Khundkar, and A. H. Zewail, "Picosecond Photofragment Spectroscopy. III. Vibrational Predissociation of van der Waals Clusters," J. Chem. Phys. **87,** 115–127 (1987).
14. J. A. Syage and J. Steadman, "Picosecond Mass-Selective Measurements of Molecular Cluster Reactions: $(CH_3I)_n$ $\tilde{A}$ State Excitation," Chem. Phys. Lett. **166,** 159–166 (1990).
15. J. Steadman and J. A. Syage, "Picosecond Mass-Selective Measurements of Phenol-$(NH_3)_n$ Acid-Base Chemistry in Clusters," J. Chem. Phys. **92,** 4630–4632 (1990).
16. J. A. Syage, "Photodissociation and Metastable Decay of Solvated Cluster Ions," J. Chem. Phys. **92,** 1804–1810 (1990); J. A. Syage and J. Steadman, "A Time-of-Flight Mass Filter for Ion and Cluster Ion Photodissociation Studies," Rev. Sci. Instrum. **61,** 1204–1210 (1990).
17. J. A. Syage, J. E. Pollard, and J. Steadman, "Resonance Ion Dissociation Spectroscopy of CH_3I^+ Produced by Molecular Beam Electron-Impact Ionization," Chem. Phys. Lett. **161,** 103–110 (1989).
18. W. C. Wiley and I. H. McLaren, "Time-of-Flight Mass Spectrometer with Improved Resolution," Rev. Sci. Instrum. **26,** 1150–1157 (1955).
19. J. A. Syage, "Measurements of Electron-Impact Ionization and Dissociation Cross Sections in a Crossed Electron-Supersonic Molecular Beam," Chem. Phys. Lett. **143,** 19–25 (1988); J. E. Pollard and R. B. Cohen, "Electron-Impact Ionization Time-of-Flight Mass Spectrometer for Molecular Beams," Rev. Sci. Instrum. **58,** 32–37 (1987).
20. C. R. Moylan and J. I. Brauman, "Gas Phase Acid-Base Chemistry," Annu. Rev. Phys. Chem. **34,** 187–215 (1983); D. F. McMillen and D. M. Golden, "Hydrocarbon Bond Dissociation Energies," Annu. Rev. Phys. Chem. **33,** 493–532 (1982).
21. P. Kebarle, "Ion Thermochemistry and Solvation from Gas Phase Ion Equilibria," Annu. Rev. Phys. Chem. **28,** 445–476 (1977); M. J. Mautner and C. V. Speller, "Filling of Solvent Shells About Ions. 1. Themochemical Criteria and the Effects of Isomeric Clusters," J. Phys. Chem. **90,** 6616–6624 (1986).
22. D. Solgadi, C. Jouvet, and A. Tramer, "Resonance Enhanced Multiphoton Ionization Spectra and Ionization Thresholds of Phenol-$(NH_3)_n$ Clusters," J. Phys. Chem. **92,** 3313–3315 (1988).
23. L. A. Bloomfield, R. R. Freeman, and W. L. Brown, "Photofragmentation of Mass-Resolved Si_{2-12}^+ Clusters," Phys. Rev. Lett. **54,** 2246–2249 (1985); Q.-P. Zhang, Y. Liu, R. F. Curl, F. K. Tittel, and R. E. Smalley, "Photodissociation of Semiconductor Positive Cluster Ions," J. Chem. Phys. **88,** 1670–1677 (1988); M. L. Alexander, M. A. Johnson, N. E. Levinger, and W. C. Lineberger, "Photodissociation of Mass-Selected $(CO_2)_n^-$ Clusters: Evaporation Leading to Magic Numbers in Fragment-Ion Distributions," Phys. Rev. Lett. **57,** 976–979 (1986).
24. L. R. Khundkar and A. H. Zewail, "Picosecond MPI Mass Spectrometry of CH_3I in the Process of Dissociation," Chem. Phys. Lett. **142,** 426–432 (1987).
25. S. P. Sapers, V. Vaida, and R. Naaman, "Multiphoton Ionization Study of Intra- and Intermolecular Effects on the Photodissociation of Methyl Iodide," J. Chem. Phys. **88,** 3638–3645 (1988); D. J. Donaldson, V. Vaida, and R. Naaman, "Ultraviolet Absorption Determination of Intracluster Predissociation Dynamics in $(CH_3I)_n$ and $(CD_3I)_n$," J. Phys. Chem. **92,** 1204–1208 (1988).